Journal of Dental Research
2015, Vol. 94(2) 312–319

DOI: 10.1177/0022034514559129
jdr.sagepub.com

NFIB Regulates Embryonic Development of Submandibular Glands

R.E. Mellas[1], H. Kim[2], J. Osinski[3], S. Sadibasic[2], R.M. Gronostajski[3], M. Cho[4], and O.J. Baker[1]

Abstract

NFIB (nuclear factor I B) is a NFI transcription factor family member, which is essential for the development of a variety of organ systems. Salivary gland development occurs through several stages, including prebud, bud, pseudoglandular, canalicular, and terminal. Although many studies have been done to understand mouse submandibular gland (SMG) branching morphogenesis, little is known about SMG cell differentiation during the terminal stages. The goal of this study was to determine the role of NFIB during SMG development. We analyzed SMGs from wild-type and *Nfib*-deficient mice ($Nfib^{-/-}$). At embryonic (E) day 18.5, SMGs from wild-type mice showed duct branching morphogenesis and differentiation of tubule ductal cells into tubule secretory cells. In contrast, SMGs from $Nfib^{-/-}$ mice at E18.5 failed to differentiate into tubule secretory cells while branching morphogenesis was unaffected. SMGs from wild-type mice at E16.5 displayed well-organized cuboidal inner terminal tubule cells. However, SMGs from $Nfib^{-/-}$ at E16.5 displayed disorganized inner terminal tubule cells. SMGs from wild-type mice at E18.5 became fully differentiated, as indicated by a high degree of apicobasal polarization (i.e., presence of apical ZO-1 and basolateral E-cadherin) and columnar shape. Furthermore, SMGs from wild-type mice at E18.5 expressed the protein SMGC, a marker for tubule secretory cells. However, SMGs from $Nfib^{-/-}$ mice at E18.5 showed apicobasal polarity, but they were disorganized and lost the ability to secrete SMGC. These findings indicate that the transcription factor NFIB is not required for branching morphogenesis but plays a key role in tubule cell differentiation during mouse SMG development.

Keywords: salivary glands, differentiation, epithelium, transcription factors, cells, morphogenesis

Submandibular gland (SMG) development requires synchronization of multiple signaling pathways to regulate cell migration, proliferation, apoptosis, and differentiation (Patel et al. 2006). These processes are regulated by the functional integration of growth factors, cytokines, and transcription factors (Jaskoll et al. 2004). Mouse SMG development involves 2 major steps: duct branching morphogenesis and acinar differentiation (Martinez 1994). Development of the mouse SMG starts at embryonic (E) E11.5 (prebud stage), a period in which epithelial cells proliferate and form a localized thickened epithelium adjacent to the developing tongue (Tucker 2007). At E12.5 (bud stage), the epithelial cells continuously proliferate, invaginate into the underlying mesenchyme, and form the epithelial bud (Tucker 2007). The epithelial bud further grows and forms a solid epithelial cord that begins branching morphogenesis (E13). Then, clefts deepen into the epithelial cord between E13 and E14.5 (pseudoglandular stage) and continue branching (Tucker 2007). The solid epithelial branches undergo lumen formation through apoptosis of the inner cells at E15.5 (canalicular stage) (Tucker 2007). Lumenization is completed and the terminal tubules inner cells become cuboidal and begin to differentiate into tubule secretory cells at E17.5 (terminal bud stage) (Tucker 2007). The terminal tubule cells become columnar and display apicobasal polarity and further differentiate into 2 transient secretory cell types; proacinar (type III) and terminal tubule (type I) cells at E18.5 (Yamashina and Barka 1972; Cutler and Chaudhry 1974). Type III cells develop into seromucous acinar cells of the mature salivary glands (Yamashina and Barka 1972; Denny et al. 1988; Moreira et al. 1991). Type I

[1]School of Dentistry University of Utah, Salt Lake City, UT, USA
[2]Department of Restorative Dentistry, School of Dental Medicine, University at Buffalo, The State University of New York, Buffalo, NY, USA
[3]Department of Biochemistry, Developmental Genomics Group, Center of Excellence in Bioinformatics and Life Science, University at Buffalo, The State University of New York, Buffalo, NY, USA
[4]Department of Oral Biology, School of Dental Medicine, University at Buffalo, The State University of New York, Buffalo, NY, USA

A supplemental appendix to this article is published electronically only at http://jdr.sagepub.com/supplemental.

Corresponding Author:
O.J. Baker, School of Dentistry, The University of Utah, 383 Colorow Dr., Room 289A, Salt Lake City, UT 84108-1201, USA.
Email: olga.baker@hsc.utah.edu

cells are thought to contribute to the formation of adult SMG intercalated ducts (Denny et al. 1988). The SMG protein C (SMGC) is present almost exclusively in type I cells throughout development (Ball and Redman 1984). However, it is also expressed in a subset of granular intercalated duct cells in adult SMGs (Zinzen et al. 2004). The role of SMGC in salivary gland development is not well understood. However, the initial expression and exocrine packaging of SMGC during development may prime terminal differentiation of salivary mucous and seromucous acinar cells (Das et al. 2009).

The nuclear factor I (NFI) gene family encodes 4 site-specific transcription factors (e.g., *Nfia, Nfib, Nfic*, and *Nfix*) that are essential for the development of a number of organ systems in mice (Gronostajski 1986, 2000). In particular, the family member nuclear factor I B (NFIB) has been shown to be essential for fetal lung maturation and brain development in mice (Steele-Perkins et al. 2005). Lung development is regulated by mesenchymal-epithelial interactions similar to the salivary glands (Cutler and Gremski 1991). Furthermore, both lungs and salivary glands share analogous branched patterns and tissue organization. Therefore, the goal of this study was to explore whether the NFIB plays a role in mouse SMG cell differentiation.

Materials and Methods

Experimental Animals

Homozygous *Nfib*-deficient ($Nfib^{-/-}$) mice were generated by removal of the second exon from the *Nfib* gene, which encodes the transcription factor NFIB DNA-binding and dimerization domain as described previously (Steele-Perkins et al. 2005). $Nfib^{-/-}$ mice were backcrossed into the C57BL/6 background, and C57BL/6 was used as a wild-type control. All animals were bred and maintained at the Laboratory Animal Facility of Roswell Park Cancer Institute. Polymerase chain reaction (PCR) genotyping was performed using $Nfib^{-/-}$ specific primers: forward: 5′-GCTGA GTTGGGAGATTGTGTC-3′ and reverse: 5′-TTCTGCTT GATTTCGGGCTTC-3′ as described previously (Steele-Perkins et al. 2005).

Gross View

Mouse embryos were collected at E18.5 and fixed overnight in 4% paraformaldehyde in phosphate-buffered saline (PBS). SMGs were dissected out from wild-type and $Nfib^{-/-}$ mice and photographed (Zeiss Axiopht photomicroscope; Carl Zeiss, Thornwood, NY, USA).

Histology

Formalin-fixed E16.5 and E18.5 SMGs were dissected out, embedded in paraffin, and stained with hematoxylin and eosin as well as 1% toluidine blue, as described previously (Lee et al. 2009). Toluidine blue specimens were prepared at the University at Buffalo Histological Services, Department of Pathology and Anatomical Sciences, by fixing and dehydrating SMGs and embedding in plastic (Epon). The blocks were then cut into 1-µm-thick sections and stained. Sections and mosaic images were obtained using a Leica DMI6000B inverted microscope (Leica Microsystems, Mannheim, Germany).

Immunohistochemistry

For 10 min, 5-µm thick deparaffinized sections were incubated in 5% urea containing 50 mM β-mercaptoethanol at 90 °C (Das et al. 2009). Sections were then incubated for 30 min in 0.3% hydrogen peroxide in methanol, 5% normal goat serum, and 1% bovine serum albumin in 1× PBS. Sections were subsequently incubated with the primary antibodies overnight at 4 °C as follows: rabbit anti-SMGC antiserum (1:1,000, a kind gift from Dr. Lily Mirels, Berkeley, CA, USA) that was raised against a bacterially expressed GST-SMGC fusion protein (Ball et al. 1993) and rabbit anti–aquaporin-5 (1:100; Santa Cruz Biotechnology, Santa Cruz, CA, USA). After incubation with peroxidase goat anti-rabbit (1:500 dilution in 5% goat serum; Santa Cruz Biotechnology) for 1 h, antigens were localized using an avidin-biotin-peroxidase complex kit (Vector Laboratories, Burlingame, CA, USA). Antibodies were diluted in 1× PBS containing 2% normal goat serum and 0.2% Triton X-100. Tissue sections were washed 3 times in 1× PBS for 5 min each between steps.

Confocal Microscopy Analyses

Formalin-fixed, paraffin-embedded mouse SMG tissue sections were deparaffinized by 3 washes for 5 min each in 100% xylene. Sections were washed twice for 5 min in 100% ethanol, twice for 5 min in 95% ethanol, and 5-min washes in 80%, 70%, and 50% ethanol. Sections were then washed twice for 5 min in distilled water. Antigen retrieval was performed by placing the slides in a pressure cooker (Nesco, Two Rivers, WI, USA) filled with 1× sodium citrate (5.98 g sodium citrate dissolved in 2 L distilled water and 0.05% Tween 20 adjusted to pH 6.0) for 6 min. Sections were allowed to cool down to room temperature and rinsed with PBS. This procedure was followed by permeabilization with 0.1% Triton X-100 (v/v) for 45 min at room temperature. Finally, sections were washed 3 times for 5 min each in 1× PBS and incubated at 4 °C for 48 h with the following primary antibodies: rabbit anti–ZO-1 (1:50 dilution in 5% goat serum; Invitrogen, Carlsbad, CA, USA) with mouse anti–E-cadherin (1:100 dilution in 5% goat serum; BD Biosciences, San Jose, CA, USA) and rabbit anti-NFIB (1:50 dilution in 5% goat serum; Sigma, St. Louis, MO, USA) with mouse anti–E-cadherin (1:100 dilution in 5%

goat serum; BD Biosciences). The following day, the slides were warmed to room temperature for 20 min and washed 3 times for 5 min each with 1× PBS. Tissue sections were incubated for 1 h with Alexa Fluor 488–conjugated goat anti-rabbit (1:500 dilution in 5% goat serum; Invitrogen), washed 3 times with 1× PBS, and incubated with phalloidin 633 (1:400 dilution in 1× PBS; Invitrogen) for 1 h. All sections were stained for 30 min with propidium iodide nucleic acid stain (1:3,000 dilution in 2× sodium citrate; Invitrogen). Images were taken using a Carl Zeiss 510 confocal microscope, and localization of proteins was visualized using the ZEN software (black edition; Carl Zeiss).

RNA Extraction and Quantitative PCR

RNA was extracted with TRIzol reagent (Invitrogen), and 2 to 5 µg was used for random hexamer primed complementary DNA (cDNA) synthesis with Superscript II (Invitrogen). Transcript levels were quantified by quantitative PCR (QPCR) with a Bio-Rad (Hercules, CA, USA) iCycler real-time PCR machine using SYBR Green as described previously (Steele-Perkins et al. 2005). All comparisons were made between homozygous mutant and wild-type littermates. All results were normalized to β2-microglobulin levels. Sequences of the primers are available upon request.

Statistical Analyses

Data are means ± SEM of results from 3 or more determinations. Data were analyzed by 1-way analysis of variance (ANOVA) followed by linear trend analysis where $P < 0.05$ represents significant differences between experimental groups.

Results

Nfib-*Deficient (*Nfib$^{-/-}$*) Mice Display SMG Hypoplasia at E18.5*

We compared the gross morphology of wild-type and *Nfib*$^{-/-}$ SMGs at E18.5. As shown in Figure 1, SMGs from wild-type mice were approximately 2.5 mm in length and 1.5 mm in width (Fig. 1A). In contrast, SMGs from *Nfib*$^{-/-}$ mice were approximately 1.5 mm in length and 1.3 mm in width (Fig. 1B). When comparing mosaic images, we observed that SMG from wild-type animals showed well-developed interlobular regions with an oblong structure (Fig. 1C). However, SMGs from *Nfib*$^{-/-}$ mice showed poorly developed lobular regions and a small round structure (Fig. 1D). The characteristics observed in SMGs from *Nfib*$^{-/-}$ mice are indicative of SMG hypoplasia (Fig. 1B, D). We were able to distinguish SMG and sublingual glands (SLGs) in the wild-type mice at E18.5 (Fig. 1C, red arrow); however, this distinction was not evident in glands from the *Nfib*$^{-/-}$ mice at the same stage or in wild-type animals at E16.5 (Fig. 1B, D). Furthermore, a complete lack of mucin expression in *Nfib*$^{-/-}$ mice and E16.5 wild-type mice was observed (Appendix Fig. 1A, B, D–F, H), indicating that the mucous component of the gland is absent in *Nfib*$^{-/-}$ mice and E16.5 wild-type mice. Mucin expression was expressed only in E18.5 wild-type glands (Appendix Fig. 1C, G, red arrow). Hematoxylin and eosin staining also showed the lack of SLGs in both the wild-type and the *Nfib*$^{-/-}$ mice at E16.5 (Appendix Fig. 2).

Submandibular Glands from Nfib$^{-/-}$ *Mouse Fail to Differentiate into Ductal Tubule Secretory Cells*

We compared histology sections from wild-type and *Nfib*$^{-/-}$ mouse SMG at E18.5 (Fig. 1E–H). Wild-type mouse SMG displayed compartmentalized lobes, which contained tree-like glandular epithelial networks surrounded by fibrous connective tissue (Fig. 1E–H). The SMG ducts were branched (Fig. 1E, G, yellow arrows) and displayed lumens in the wild-type mouse SMG at E18.5 (Fig. 1E, G, red arrows). Although the *Nfib*$^{-/-}$ mouse SMG showed canaliculized ducts and branching (Fig. 1F, H, yellow arrows), it lacked tubule secretory cells, and ducts were connected directly with terminal buds (i.e., displayed poor lumen formation) (Fig. 1F, H, aquamarine arrow). Wild-type SMG at E18.5 displayed ductal terminal tubule cells that were connected with tubule secretory cells (Fig. 1G, green arrow). The tubule secretory cells in SMGs from wild-type mice at E18.5 were terminated with proacinar type III cells (Fig. 1G).

The toluidine blue–stained sections showed each terminal tubule lined with well-polarized and differentiated tubule secretory cells with numerous secretory granules (Fig. 2A, red arrows) and some individual secretory cells (Fig. 2A, inset a, red arrow) in SMGs from wild-type mice at E18.5 but not at E16.5 (Fig. 2B, note the darkly stained tubular cells). In contrast, each terminal tubule of the *Nfib*$^{-/-}$ mouse SMG at E18.5 ended with a terminal bud, thereby completely lacking tubule secretory cells (Fig. 2C, aquamarine arrow) similar to what we observed with *Nfib*$^{-/-}$ mouse SMG at E16.5 (Fig. 2D). The end terminal bud cells observed in the *Nfib*$^{-/-}$ mouse SMG at E18.5 and E16.5 displayed a polygonal shape and were randomly distributed in a short stalk that was distal to the terminal bud (Fig. 2C, D). We also observed some proacinar cells located at the distal end of the bud in the *Nfib*$^{-/-}$ mouse SMG at E18.5 (Fig. 2C, yellow arrow). We observed that the *Nfib*$^{-/-}$ mouse SMG at E18.5 appeared to have more connective tissue than the wild-type mouse SMG at E18.5 (Fig. 2C and 2A, respectively). In general, these images show the presence of secretory granules and lumen formation in wild-type SMG and the absence of secretory granules and lumen formation in the *Nfib*$^{-/-}$ mouse SMG. Also, SMGs from *Nfib*$^{-/-}$ mice at E18.5 showed signs of underdeveloped lobules lacking tubule secretory cells compared with wild-type mouse SMGs.

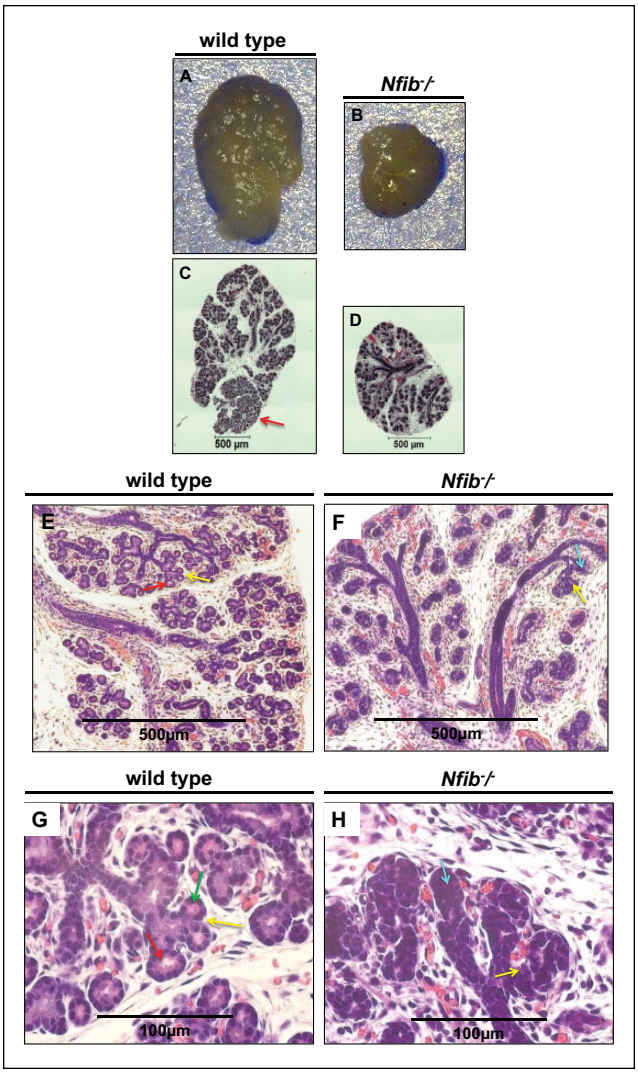

Figure 1. The *Nfib*$^{-/-}$ mouse submandibular gland (SMG) at E18.5 displays signs of salivary gland hypoplasia and poor acinar lumen formation. Salivary glands were dissected for gross view and/or embedded in paraffin and stained with hematoxylin and eosin as described in the Materials and Methods. SMGs from the *Nfib*$^{-/-}$ mouse display a noticeable decrease in size and poor lobule formation compared with SMGs from wild-type mice (**A**, **B**). These characteristics were more evident in the stained SMG sections that indicate salivary branching morphogenesis in both groups. However, an absence of acinar lumens in the *Nfib*$^{-/-}$ mouse was evident (**C**, **D**). Shown at 10× are SMGs from the wild-type and *Nfib*$^{-/-}$ mice (**E**, **F**). The images were magnified to 40× to show specific details (**G**, **H**). SMG from the wild-type mouse at E18.5 exhibits branched and canaliculized ducts that are continuous and display lumen formation (E, red arrow). The SMG from *Nfib*$^{-/-}$ mouse shows complete branched and canaliculized ducts (F, H, yellow arrows) but lacks tubule secretory cells and ducts are connected directly with terminal buds (i.e., poor lumen formation) (F, aquamarine arrow). The wild-type SMG at E18.5 also displays ductal terminal tubule cells that are connected with tubule secretory cells (G, green arrow).

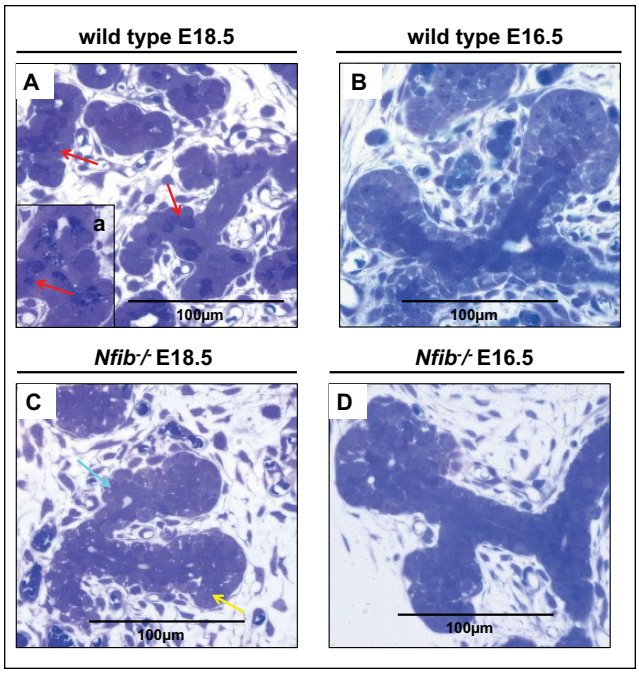

Figure 2. The *Nfib*$^{-/-}$ mouse submandibular glands (SMGs) at E16.5 and E18.5 lack tubule secretory cells. Salivary glands were dissected, embedded in paraffin, and stained with toluidine blue as described in the Materials and Methods. In the wild-type mouse SMG at E18.5, there are fully differentiated tubule secretory cells located between duct and proacinar cells. These secretory cells contain numerous secretory granules (**A**, red arrows) as well as some individual secretory cells (A, inset a, red arrow). In the wild-type mouse SMG at E16.5, the inner duct tubule cells are darkly stained, cuboidal in shape, and aligned in a row (**B**). In the *Nfib*$^{-/-}$ mouse SMG at E18.5, the inner tubule cells failed to differentiate and the overall morphology of terminal buds resemble those from the wild-type mouse at E16.5. Also, in E18.5 *Nfib*$^{-/-}$ mouse SMG, the proacinar cells are located at the distal end of the bud (**C**, yellow arrow) and lack secretory granules (C, aquamarine arrow). In the *Nfib*$^{-/-}$ mouse SMG at E16.5, the inner duct tubule cells are polygonal in shape and disorganized (**D**).

Submandibular Glands from the Nfib$^{-/-}$ *Mouse Do Not Express SMGC and Aquaporin 5*

We compared the secretory machinery between wild-type and *Nfib*$^{-/-}$ mouse SMG at E18.5 (Fig. 3A, B). As shown in Figure 3A (red arrows), wild-type mouse SMG at E18.5 displayed lumen formation and apical expression of the water channel, aquaporin 5. In contrast, *Nfib*$^{-/-}$ mouse SMG at E18.5 did not show apical aquaporin 5 and failed to form lumens or, in some instances, formed poor lumens (Fig. 3B, yellow arrows).

We also observed in wild-type SMG at E18.5 that the secretory protein SMGC was apically expressed in terminal tubule secretory cells but was absent in proacinar and tubule

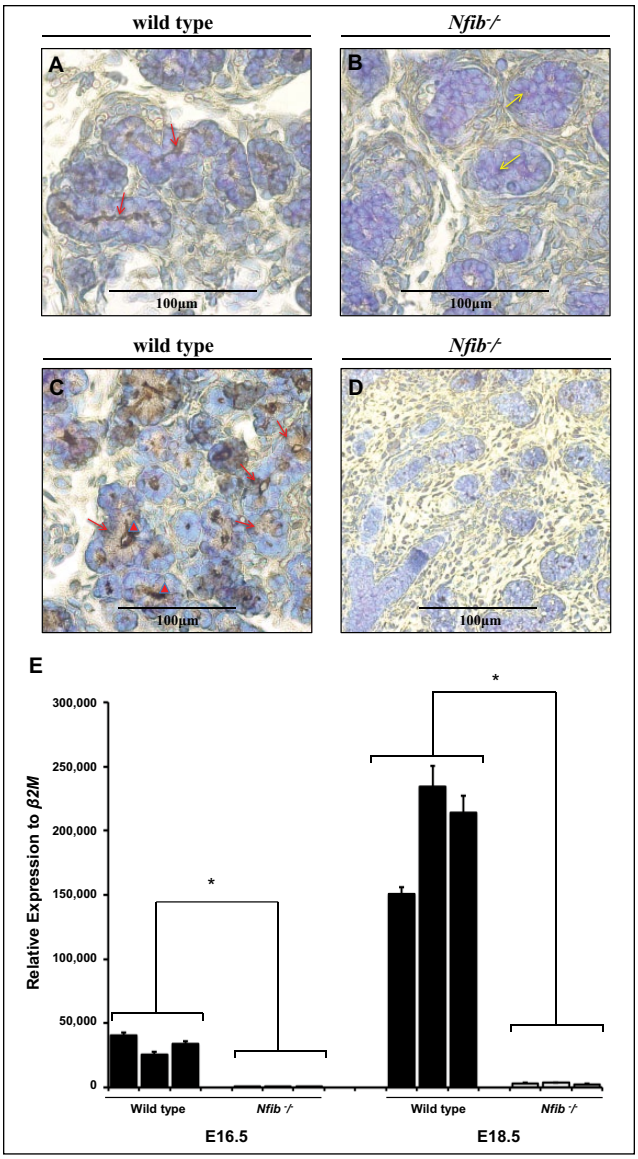

Figure 3. The *Nfib*$^{-/-}$ mouse submandibular gland (SMG) at E18.5 lack aquaporin 5 and SMG protein C (SMGC) expression. Salivary glands were dissected, embedded in paraffin, and stained with aquaporin 5 or SMGC antibodies as described in the Materials and Methods. Strong aquaporin 5 immunohistochemical localization along the luminal membrane of the tubule secretory cells from wild-type mouse SMG was observed (**A**, red arrows). However, there was an absence of immunohistochemical staining for aquaporin 5 in the terminal buds of the *Nfib*$^{-/-}$ mouse SMG and failure to form lumens (or displayed poorly formed lumens) (**B**, yellow arrows). (B) Strong SMGC immunohistochemical localization in the supranuclear region (**C**, red arrows) and in the lumen of tubule secretory cells (C, red arrowheads) from wild-type mouse SMG was observed. However, no immunostaining in the proacinar cells of the wild-type SMG was observed (C). There was an absence of immunohistochemical staining for SMGC in the terminal buds of the *Nfib*$^{-/-}$ mouse SMG (**D**). (Figures 3C and 3D were taken at 20×.) Quantitative polymerase chain reaction analyses for SMGC were performed in wild-type and *Nfib*$^{-/-}$ mouse SMG at E16.5 and E18.5 (**E**). Numbers on the x-axis represent litter records. Data represent the means ± SEM of results from 3 experiments, where $*P < 0.05$ represents significant differences from wild-type mouse.

cells (Fig. 3C, red arrows). The *Nfib*$^{-/-}$ mouse SMG at E18.5 showed an absence of staining for SMGC throughout the gland (Fig. 3D). Results from the QPCR analysis showed that SMGC transcript expression from wild-type mouse SMG is significantly decreased at E16.5 compared with E18.5 (Fig. 3E). These results corroborate the immunohistochemistry studies indicating that SMGC protein expression is absent in *Nfib*$^{-/-}$ mouse SMG.

SMGs from the Nfib$^{-/-}$ *Mouse Exhibit Normal Cell Polarity but Altered ZO-1 Organization and Lack Expression of the Protein NFIB*

We compared the expression of apical and basolateral markers in wild-type and *Nfib*$^{-/-}$ mouse SMG at E16.5 and E18.5 (Fig. 4A–H). As shown in Figure 4A, wild-type mouse SMG at E16.5 displayed apical expression of the tight junction protein ZO-1 (green) and basolateral expression of the adherens junction protein, E-cadherin (red). Furthermore, we observed apical lumen formation (Fig. 4A, B, aquamarine arrows). However, the *Nfib*$^{-/-}$ mouse SMG at E16.5 displayed disorganized apical ZO-1 and poor lumen formation, and the cells appeared to be in a disorganized arrangement (Fig. 4C, D). The *Nfib*$^{-/-}$ mouse SMG expressed E-cadherin at the same time period (Fig. 4C, D); however, it appeared reduced compared with E-cadherin in the wild-type mouse SMG (Fig. 4A, B). Wild-type mouse SMG at E18.5 displayed cell polarity and a round lumen in most of the acinar and ductal structures (Fig. 4E, F, aquamarine arrows). Interestingly, the *Nfib*$^{-/-}$ mouse SMG at E18.5 also expressed E-cadherin and displayed cell polarity, but there was absence of lumens in both acinar and ductal structures (Fig. 4G, H). Appendix Figure 3 shows differentiation between ductal lumen formation and terminal end buds lumen formation, which can be noted by red and yellow arrows, respectively. As shown in Figure 4I–L, we corroborated that the NFIB was absent in SMG cells of *Nfib*$^{-/-}$ mice. Wild-type mouse SMG at E18.5 expressed the NFIB protein in the nucleus of all cell types (Fig. 4I, J). However, we observed only nonspecific staining in SMGs from *Nfib*$^{-/-}$ mice at E18.5, suggesting an absence of the NFIB protein (Fig. 4K, L and Appendix Fig. 4).

Discussion

In this study, we demonstrated that SMGs from *Nfib*$^{-/-}$ mice develop normally until terminal tubules are formed, suggesting that the transcription factor NFIB has little or no effect on the initial bud formation, branching morphogenesis, and canaliculation during SMG development (see Appendix Fig. 2). However, *Nfib* inactivation caused failure in terminal tubule formation at E16.5 and tubule cell differentiation at E18.5 (Figs. 1, 2). The terminal tubules appear transiently during embryonic SMG development, as they develop into intercalated ducts during postnatal SMG development (Ball and Nelson 1978). Likewise, proacinar cells differentiate into acinar cells right after birth (Moreira

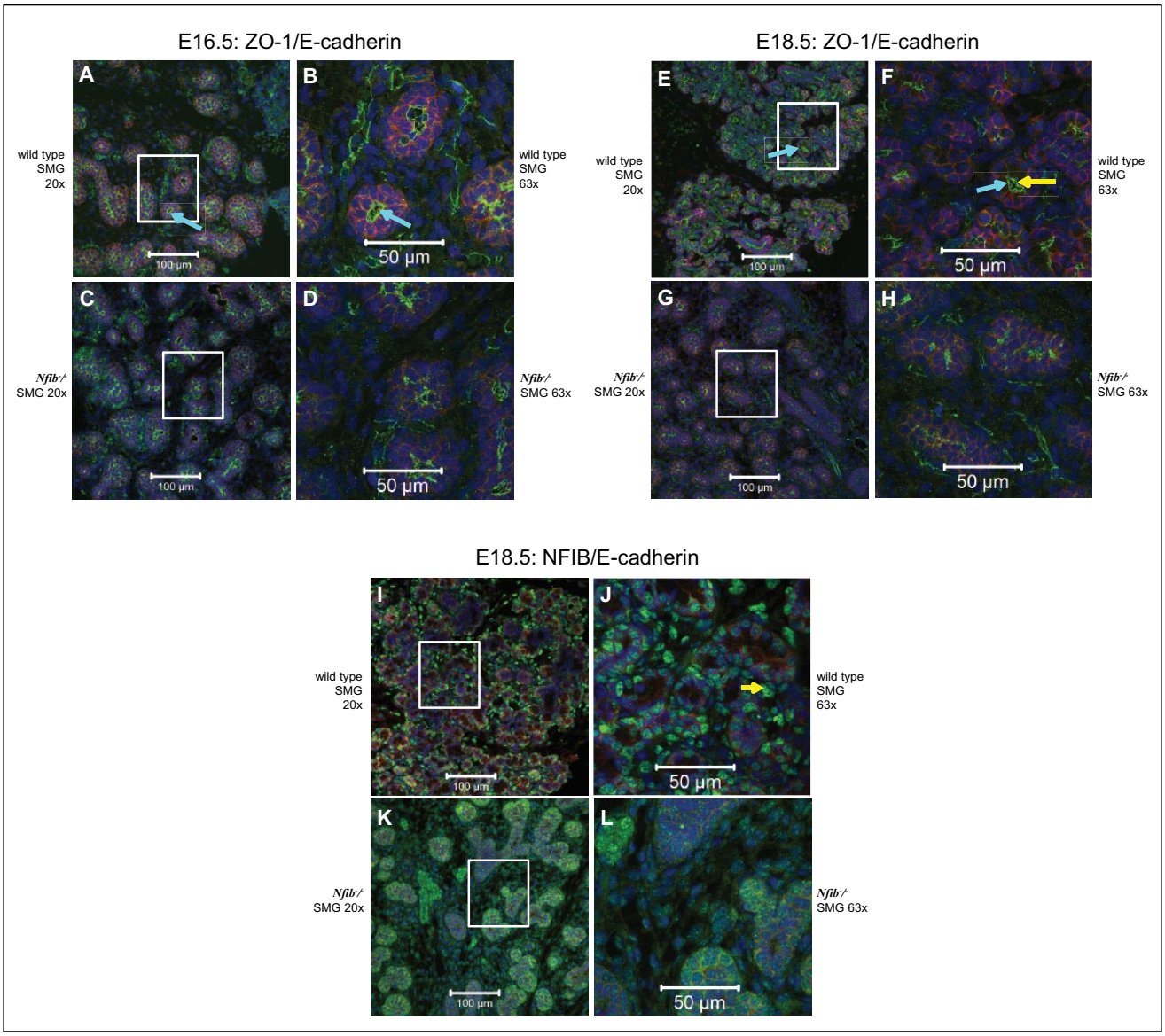

Figure 4. The *Nfib*$^{-/-}$ mouse submandibular gland (SMG) exhibits normal cell polarity but altered ZO-1 organization and does not express the nuclear factor I B (NFIB). Salivary glands were dissected, embedded in paraffin, and stained with ZO-1 (green), NIFB (green), E-cadherin (red) antibodies, and propidium iodide (blue) as described in the Materials and Methods. Shown are confocal images of acinar and ductal cells from SMG tissue sections at both 20× (**A**, **C**, **E**, **G**, **I**, **K**) and 63× (**B**, **D**, **F**, **H**, **J**, **L** maximum intensity projection of a z-stack). Note that ZO-1 and E-cadherin maintain polarity (e.g., apical ZO-1 and basolateral E-cadherin) in SMG from both wild-type and *Nfib*$^{-/-}$ mice at E16.5 (A–D) and E18.5 (E–H). However, the lumen is well developed in wild-type mouse SMG at E18.5 (F, yellow arrow) compared with *Nfib*$^{-/-}$ mouse at E18.5 (H), which lacks lumen formation. Aquamarine arrows (A, B, E, and F) show apical lumen formation. SMG from the wild-type mouse at E18.5 express the NFIB protein in the nucleus of all cell types (I and J, yellow arrow). The *Nfib*$^{-/-}$ mouse SMG lack NFIB protein expression (K and L).

et al. 1990; Moreira et al. 1991). Therefore, it is apparent that intercalated ducts (the smallest structures connected directly to the acini) are formed as part of the secretory unit rather than as ducts. Consequently, NFIB must play a key role in the development of this secretory unit. The *Nfib*$^{-/-}$ mice die immediately after birth due to incomplete lung development (Steele-Perkins et al. 2005), and thus the role of *Nfib* inactivation on postnatal SMG could not be investigated in the present study. Future studies using localized targeting of NFIB in SMG will be able to determine whether it regulates the differentiation of acinar cells after birth.

Previous studies demonstrated that the mesenchyme regulates branching morphogenesis in a salivary gland–type specific manner (Lawson 1972; Ball 1974; Nogawa and Mizuno 1981), but mesenchyme failed to control terminal acinar cell differentiation (Lawson 1972; Sakakura et al. 1976). Other studies demonstrated that rat SMG at E16.5 (pseudoglandular stage) cultured after removal of

mesenchyme failed to branch but differentiated into acinar cells (Cutler 1980; Cutler and Gremski 1991). These studies support the notion that NFIB might play a role in epithelial cell differentiation but not mesenchyme (as SMG from *Nfib*$^{-/-}$ mice maintain branching). However, ectoderm-mesoderm interactions are essential for the formation of several structures that arise from the ectoderm, including salivary glands (Jaskoll et al. 2003). Interestingly, a study demonstrated that mesenchymal NFIB regulates both mesenchymal and epithelial cell proliferation through multiple pathways essential for the maturation of distal lung epithelium (Hsu et al. 2011). Therefore, future studies evaluating the role of NFIB in SMG mesenchyme will be necessary.

We have demonstrated that the *Nfib*$^{-/-}$ mouse represents a valuable model to understand salivary gland development. Particularly, it would be useful to determine whether NFIB controls genes involved in salivary gland developmental disorders such as hypohidrotic ectodermal dysplasia (Okumura et al. 2012). Patients with ectodermal dysplasia fail to express ectodysplasin (*EDA*) or the ectodysplasin receptor (*EDAR*). The EDA/EDAR signaling pathway is essential for the mesoderm-ectoderm interaction that controls the formation of ectodermal structures such as the skin, hair follicles, sweat glands, and teeth (Jaskoll et al. 2003). The EDA/EDAR proteins localize in SMG epithelia at the site of lumen formation after the pseudoglandular stage and are essential for lumen formation and histodifferentiation of the epithelia (Jaskoll et al. 2003).

The *Nfib*$^{-/-}$ mouse model is also useful to understand signaling pathways that have the potential to control certain pathological conditions of the salivary glands. For instance, *NFIB* is a frequent translocation partner of *HMGA2* in salivary gland pleomorphic adenoma and mucoepidermoid carcinoma (Von Holstein et al. 2012; Stenman 2013). In addition, *NFIB* fusions with *MYB* transcripts are present in adenoid cystic carcinomas of the breast, salivary, and lacrimal glands (Persson et al. 2009; Stenman 2013). A recent study of the mutational landscape of adenoid cystic carcinomas also revealed mutations of *Nfib* in a subset of tumors (Ho et al. 2013). Taken together, these studies indicate that alterations of *Nfib* gene and protein expression lead to oncogenic properties and are involved in both lacrimal and salivary gland tumors, as well as in lung and breast cancer.

In summary, our findings indicate that the transcription factor NFIB does not interfere with branching morphogenesis but plays a key role in tubule cell differentiation during mouse SMG development. Because duct secretory cells are developed after completion of ductal branching, and their formation is hindered completely in the *Nfib*$^{-/-}$ SMG, this indicates that NFIB also plays a key role in duct secretory cell development. Future studies will be necessary to determine a role of NFIB in the salivary gland mesenchyme. Our model might prove useful to understand NFIB signaling and allow targeting of developmental diseases or pathological conditions of the salivary glands.

Author Contributions

R.E. Mellas, M. Cho, O.J. Baker, contributed to conception, design, data acquisition, analysis, and interpretation, drafted and critically revised the manuscript; H. Kim, J. Osinski, S. Sadibasic, contributed to data acquisition and analysis, drafted the manuscript; R.M. Gronostajski, contributed to conception, design, data acquisition, analysis, and interpretation, critically revised the manuscript. All authors gave final approval and agree to be accountable for all aspects of the work.

Acknowledgments

We acknowledge Dr. Wade J. Sigurdson, Director of the Confocal Microscopy and 3-Dimensional Imaging Core Facility of the School of Medicine and Biomedical Sciences, The State University of New York at Buffalo (UB), for assistance in imaging of specimens, and Nicholas Pappas for providing the data on mucin staining. This work was supported by the National Institutes of Health (NIH)–National Institute of Dental and Craniofacial Research (NIDCR) grants R01DE022971 and R01DE021697 (to OJB) and NIH/National Heart, Lung, and Blood Institute (NHLBI) grant HL080624 (to RG). We thank Dr. Lily Mirels (Biology Department, University of California, San Diego, La Jolla, CA) for the generous gift of rabbit anti-SMGC serum. The authors declare no potential conflicts of interest with respect to the authorship and/or publication of this article.

References

Ball WD. 1974. Development of the rat salivary glands: 3. Mesenchymal specificity in the morphogenesis of the embryonic submaxillary and sublingual glands of the rat. J Exp Zool. 188(3):277–288.

Ball WD, Hand AR, Moreira JE, Iversen JM, Robinovitch MR. 1993. The B1-immunoreactive proteins of the perinatal submandibular gland: similarity to the major parotid gland protein, RPSP. Crit Rev Oral Biol Med. 4(3–4):517–524.

Ball WD, Nelson NJ. 1978. A stage-restricted secretory system in the submandibular gland of the neonatal rat. Differentiation. 10(3):147–158.

Ball WD, Redman RS. 1984. Two independently regulated secretory systems within the acini of the submandibular gland of the perinatal rat. Eur J Cell Biol. 33(1):112–122.

Cutler LS. 1980. The dependent and independent relationships between cytodifferentiation and morphogenesis in developing salivary-gland secretory-cells. Anat Rec. 196(3):341–347.

Cutler LS, Chaudhry AP. 1974. Cytodifferentiation of the acinar cells of the rat submandibular gland. Dev Biol. 41(1):31–41.

Cutler LS, Gremski W. 1991. Epithelial-mesenchymal interactions in the development of salivary glands. Crit Rev Oral Biol Med. 2(1):1–12.

Das B, Cash MN, Hand AR, Shivazad A, Culp DJ. 2009. Expression of Muc19/Smgc gene products during murine sublingual gland development: cytodifferentiation and maturation of salivary mucous cells. J Histochem Cytochem. 57(4):383–396.

Denny PA, Pimprapaiporn W, Kim MS, Denny PC. 1988. Quantitation and localization of acinar cell–specific mucin in submandibular glands of mice during postnatal development. Cell Tissue Res. 251(2):381–386.

Gronostajski RM. 1986. Analysis of nuclear factor I binding to DNA using degenerate oligonucleotides. Nucleic Acids Res. 14(22):9117–9132.

Gronostajski RM. 2000. Roles of the NFI/CTF gene family in transcription and development. Gene. 249(1–2):31–45.

Ho AS, Kannan K, Roy DM, Morris LG, Ganly I, Katabi N, Ramaswami D, Walsh LA, Eng S, Huse JT, et al. 2013. The mutational landscape of adenoid cystic carcinoma. Nat Genet. 45(7):791–798.

Hsu YC, Osinski J, Campbell CE, Litwack ED, Wang D, Liu S, Bachurski CJ, Gronostajski RM. 2011. Mesenchymal nuclear factor I B regulates cell proliferation and epithelial differentiation during lung maturation. Dev Biol. 354(2):242–252.

Jaskoll T, Leo T, Witcher D, Ormestad M, Astorga J, Bringas P Jr, Carlsson P, Melnick M. 2004. Sonic hedgehog signaling plays an essential role during embryonic salivary gland epithelial branching morphogenesis. Dev Dyn. 229(4):722–732.

Jaskoll T, Zhou YM, Trump G, Melnick M. 2003. Ectodysplasin receptor-mediated signaling is essential for embryonic submandibular salivary gland development. Anat Rec A Discov Mol Cell Evol Biol. 271(2):322–331.

Lawson KA. 1972. The role of mesenchyme in the morphogenesis and functional differentiation of rat salivary epithelium. J Embryol Exp Morphol. 27(3):497–513.

Lee DS, Park JT, Kim HM, Ko JS, Son HH, Gronostajski RM, Cho MI, Choung PH, Park JC. 2009. Nuclear factor I-C is essential for odontogenic cell proliferation and odontoblast differentiation during tooth root development. J Biol Chem. 284(25):17293–17303.

Martinez JR. 1994. Developmental aspects of fluid and electrolyte secretion in salivary glands. Crit Rev Oral Biol Med. 5(3–4):281–290.

Moreira JE, Ball WD, Mirels L, Hand AR. 1991. Accumulation and localization of two adult acinar cell secretory proteins during development of the rat submandibular gland. Am J Anat. 191(2):167–184.

Moreira JE, Hand AR, Ball WD. 1990. Localization of neonatal secretory proteins in different cell types of the rat submandibular gland from embryogenesis to adulthood. Dev Biol. 139(2):370–382.

Nogawa H, Mizuno T. 1981. Mesenchymal control over elongating and branching morphogenesis in salivary-gland development. J Embryol Exp Morphol. 66:209–221.

Okumura K, Shinohara M, Endo F. 2012. Capability of tissue stem cells to organize into salivary rudiments. Stem Cells Int. 2012:502136.

Patel VN, Rebustini IT, Hoffman MP. 2006. Salivary gland branching morphogenesis. Differentiation. 74(7):349–364.

Persson M, Andrén Y, Mark J, Horlings HM, Persson F, Stenman G. 2009. Recurrent fusion of MYB and NFIB transcription factor genes in carcinomas of the breast and head and neck. Proc Natl Acad Sci U S A. 106(44):18740–18744.

Sakakura T, Nishizuka Y, Dawe CJ. 1976. Mesenchyme-dependent morphogenesis and epithelium-specific cytodifferentiation in mouse mammary-gland. Science. 194(4272):1439–1441.

Steele-Perkins G, Plachez C, Butz KG, Yang G, Bachurski CJ, Kinsman SL, Litwack ED, Richards LJ, Gronostajski RM. 2005. The transcription factor gene *Nfib* is essential for both lung maturation and brain development. Mol Cell Biol. 25(2):685–698.

Stenman G. 2013. Fusion oncogenes in salivary gland tumors: molecular and clinical consequences. Head Neck Pathol. 7(Suppl 1):S12–S19.

Tucker AS. 2007. Salivary gland development. Semin Cell Dev Biol. 18(2):237–244.

Von Holstein SL, Fehr A, Heegaard S, Therkildsen MH, Stenman G. 2012. CRTC1-MAML2 gene fusion in mucoepidermoid carcinoma of the lacrimal gland. Oncol Rep. 27(5):1413–1416.

Yamashina S, Barka T. 1972. Localization of peroxidase activity in the developing submandibular gland of normal and isoproterenol-treated rats. J Histochem Cytochem. 20(11):855–872.

Zinzen KM, Hand AR, Yankova M, Ball WD, Mirels L. 2004. Molecular cloning and characterization of the neonatal rat and mouse submandibular gland protein SMGC. Gene. 334:23–33.